



Measuring the Critical Temperature of Superconductors: A Precursor to Periodic Nanopatterning

THESIS

submitted in partial fulfillment of the
requirements for the degree of

BACHELOR OF SCIENCE

in

PHYSICS

Author : Ringo R. Groenewegen
Student ID : s1761293
Supervisor : Milan P. Allan
2nd corrector : Jan van Ruitenbeek

Leiden, The Netherlands, July 2, 2018

Measuring the Critical Temperature of Superconductors: A Precursor to Periodic Nanopatterning

Ringo R. Groenewegen

Huygens-Kamerlingh Onnes Laboratory, Leiden University
P.O. Box 9500, 2300 RA Leiden, The Netherlands

July 2, 2018

Abstract

Prior research has demonstrated by theory and simulation that the creation of holes in two-dimensional superconductors by periodic nanopatterning can increase the critical temperature. To test this theory it must be implemented experimentally and the resulting critical temperature must be measured. Preceding the modification of these superconductors, the cryogenic resistance-temperature measurement must be tested and optimized. This thesis discusses the steps, and the problems in them, of the measurement process and provides possible explanations and solutions.

Contents

1	Introduction: Purpose of the Research	6
2	Theory	8
2.1	BCS Theory: A Theory of Superconductors	8
2.1.1	Basics of BCS Theory	8
2.1.2	BLF Hamiltonian: A Simple Model	9
2.2	Modulation of Superconductors by Periodic Nanopatterning	11
2.3	Impedance and Phasors	12
2.4	Four-terminal Resistance Measurement	14
3	Experimental Procedure	19
3.1	Outline of the Production Process	19
3.2	Production Techniques	21
3.2.1	Preparing a Substrate	21
3.2.2	Exfoliation and Reactive Ion Etching	21
3.2.3	Electron Beam Lithography (EBL)	23
3.2.4	EBL Overlay	26
3.2.5	Sputtering and Lift-off	32
3.2.6	Wire Bonding	34
3.2.7	PPMS	37
4	Results	40
4.1	PPMS Measurement of NbSe ₂	40
4.1.1	Resistance-Temperature Measurement	40
4.1.2	Phase Measurement	43
4.2	Flake Thickness Measurement	45
5	Conclusion: Outlook and Further Research	47

6 Appendix	48
6.1 Diagonalization of the BLF Hamiltonian	48

Chapter 1

Introduction: Purpose of the Research

At first glance superconductors would seem to be the solution to all our energy problems - the applications of zero energy and information loss are endless. Unsurprisingly, as is always the case in nature, if something seems too good to be true, that's most likely because it is. In the case of superconductors: while their property of zero resistance reflects an ideal, friction-less world, they are incredibly impractical to use. In the current state of conventional superconductors liquid helium is generally required to cool below 30K, where most superconductors enter the superconducting state. High-temperature superconductors exist but their physical properties make them very difficult to use: most are very brittle, for example, making it impossible to turn them into wires. It's therefore not hard to imagine that there is abundant interest in getting conventional superconductors at higher temperatures.

While some researchers are creating new superconducting compounds by chemical processes, others are altering the conditions of superconductors, such as putting them under extreme pressure to increase the transition temperature. Another method for increasing the transition temperature was proposed by Milan Allan and Mark Fischer [1]. They demonstrated through theory and simulations that creating particular periodic structures of holes in a two-dimensional superconducting resulted in a higher transition temperature. This process increases the size of the unit cells of the lattice. If the holes have the correct size, shape, and configuration they are able to increase the transition temperature.

This effect which raises the transition temperature has only been simulated so the next step is to realize this concept in practice. It is not uncom-

mon for theories to be rejected because they cannot be realized in an experiment: there are limitations to the real world. To apply this in practice different configurations of holes need to be created in thin-film superconductors. Subsequently the transition temperature needs to be measured to determine if the superconductor has improved. Before holes are created, however, it needs to be verified that this measurement process is reliable. It would be pointless to spend time on creating different configurations of holes if the change in transition temperature cannot be measured.

Before creating holes in a thin film superconductor the measurement process must be analyzed. It is a long process to measure the transition temperature but these steps will be outlined in this thesis. The results of each step will be discussed and possible improvements will be presented. To demonstrate the results of the process, a final measurement is conducted on a sample and these results are analyzed.

Chapter 2

Theory

2.1 BCS Theory: A Theory of Superconductors

2.1.1 Basics of BCS Theory

Superconductivity is a thermodynamic phase of certain materials with characteristic properties such as zero resistance and the expulsion of magnetic fields. The theory of conventional superconductors (which does not include high temperature superconductors) is BCS (Bardeen-Cooper-Schrieffer) theory whose predictions match up well with the experimental results. Among others, the theory can accurately predict the following properties:

1. **Critical temperature:** this is the temperature at which the material undergoes a phase transition to its superconducting state.
2. **Energy gap:** superconductors have zero resistance because there is a large energy gap. This means that a large excitation energy is needed to break the coupled electrons apart which are the cause of superconductivity. Once the electrons have gained sufficient energy to jump the energy gap, i.e. the current is larger than the critical current, superconductivity breaks down and the resistance ceases to be zero.
3. **Critical field:** superconductors expel magnetic fields with a field strength lower than the critical field. Passed this point superconductivity breaks down and it will no longer act as a perfect diamagnet.

It took a long time for a theory of superconductivity to be developed. This is because it requires three nontrivial insights [2]:

1. **The effective force between electrons in a lattice can sometimes be attractive rather than repulsive.** While free electrons repel according to the Coulomb force, in a lattice electrons move along with a surrounding hole, together known as a quasiparticle. Quasiparticles experience highly reduced repulsion due to screening. In addition to this there is an attraction between electrons via phonons: the motion of an electron causes the positive ions in the lattice to respond by moving towards the electron. Another electron will experience a force due to the motion of these positive ions, resulting in an indirect/effective force between electrons.
2. **Two electrons mutually attracted by an arbitrarily small force outside an occupied Fermi surface become a stable pair, resulting in a bound state.** Cooper demonstrated this by showing that the electron pair has a nonzero binding energy if they can interact with an energy in the range ϵ_F to $\epsilon_F + \hbar\omega_D$, i.e. between the Fermi surface and the Debye energy which is the most likely energy of a phonon.
3. **A many-particle wave function can be constructed for the entire system which pairs up electrons near the Fermi surface.** This wave function becomes a coherent state similar to the state of a quantum fluid where the entire system can be described as a single entity.

2.1.2 BLF Hamiltonian: A Simple Model

Superconductivity arises from the interaction between electrons and phonons. The mathematical description of the interaction between these particles is generally quite complex, so simplifications exist which still give an intuitively insightful result. Some properties of superconductivity can be derived from these simplified descriptions but doing so is rather difficult and shall therefore not be demonstrated here. One such simplification is the BLF Hamiltonian which is based on the tight binding model where the hopping term t roughly indicates the energy gained by an electron as it hops between neighboring atoms. The BLF Hamiltonian is as follows:

$$H = \sum_i \frac{\mathbf{p}_i^2}{2m} + \sum_{\langle ij \rangle} \frac{1}{2} \kappa (\mathbf{u}_i - \mathbf{u}_j)^2 - \sum_{\langle ij \rangle} (t_{ij} - \boldsymbol{\alpha} \cdot (\mathbf{u}_i - \mathbf{u}_j)) (c_i^\dagger c_j + c_j^\dagger c_i) \quad (2.1)$$

The sums over $\langle ij \rangle$ indicate that the contribution of neighboring atoms i and j is added up. The first two terms are respectively the kinetic energy of

the ions and potential energy due to repulsion of the ions in the lattice. The third term contains the energy of the electrons and the electron-phonon interaction. This term is rather intuitive: the energy gained by an electron as it hops from one ion to a neighboring one reduces as the distance between the ions increases. The operators c_i^\dagger and c_j are given in second quantization and respectively indicate the creation of an electron at position i and the annihilation of an electron at position j , i.e. an electron "hops" from j to i .

To make this Hamiltonian more transparent we can diagonalize it by transforming our coordinates to (reciprocal) k -space. This is demonstrated for each of the constituent parts of the BLF Hamiltonian in Appendix 6.1. For a one-dimensional monoatomic chain the resulting diagonalized Hamiltonian is as follows [3]:

$$H = -2t \sum_k \cos(ka) c_k^\dagger c_k + \sum_k 2\hbar \sqrt{\frac{\kappa}{m} \sin^2\left(\frac{ka}{2}\right)} \left(a_k^\dagger a_k + \frac{1}{2} \right) \quad (2.2)$$

$$- \frac{4i\alpha}{\sqrt{N}} \sum_{k,q} \sin\left(\frac{qa}{2}\right) \cos(ka) u_q c_{k+q/2}^\dagger c_{k-q/2} \quad (2.3)$$

Or as written in a more comprehensible manner:

$$H = \sum_k \left[\epsilon_k c_k^\dagger c_k + \hbar\omega_k \left(a_k^\dagger a_k + \frac{1}{2} \right) - \sum_q \frac{g(k,q)}{\sqrt{N}} u_q c_{k+q/2}^\dagger c_{k-q/2} \right] \quad (2.4)$$

The first term is the energy of the electrons, the second is the phonon energy, and the third is the electron-phonon interaction. In this equation new terms have been defined:

1. $\epsilon_k = -2t \cos(ka)$: the energy of an electron with wavevector k .
2. $\omega_k = \sqrt{\frac{\kappa}{m}} \sin\left(\frac{ka}{2}\right)$: the frequency of a phonon with wavevector k . This can be seen as the frequency of oscillation of a harmonic oscillator.
3. $g(k,q) = -4i\alpha \sin\left(\frac{qa}{2}\right) \cos(ka)$: the electron-phonon coupling amplitude.

This diagonalized form of the BLF Hamiltonian with these redefined terms makes the system much more transparent and intuitive. It is now simply a sum over the energy of electrons and quantum harmonic oscillators

(phonons) at each k value and their interaction. The interaction term sums over q which are the possible phonons that can be exchanged between electrons, where one of the two loses $\hbar q$ from its crystal momentum while the other one gains it.

2.2 Modulation of Superconductors by Periodic Nanopatterning

As can be derived using BCS theory the calculation of the critical temperature of a superconductor goes according to the following equation:

$$k_B T_c = 1.13 \hbar \omega_D e^{-\frac{1}{\lambda}} \quad (2.5)$$

Clearly the critical temperature T_c increases with the parameter λ which is a material specific parameter as calculated by:

$$\lambda = \sum_{\mathbf{q}} \frac{2}{\omega_{\mathbf{q}} N(0)} \sum_{\mathbf{k}} |M_{\mathbf{k}, \mathbf{k}+\mathbf{q}}|^2 \delta(\epsilon_{\mathbf{k}}) \delta(\epsilon_{\mathbf{k}+\mathbf{q}}) \quad (2.6)$$

The Fermi energy of the system is defined to be zero. The meaning of the terms in the equation are now described:

- $\omega_{\mathbf{q}}$: the dispersion relation for the exchanged phonons which gives the frequency of an oscillation at each wavevector.
- $N(0)$: the electron density of states at the Fermi level (where $\epsilon_F = 0$). This is important because it determines the number of Cooper pairs that can be created.
- $M_{\mathbf{k}, \mathbf{k}+\mathbf{q}}$: these are the matrix elements of the electron scattering matrix. It gives the amplitude of an electron scattering from wavevector \mathbf{k} to $\mathbf{k} + \mathbf{q}$. When we compare this to the monoatomic chain from the previous section we see that in one dimension $M_{\mathbf{k}, \mathbf{k}+\mathbf{q}} \rightarrow g(k, q)$.
- $\delta(\epsilon_{\mathbf{k}}) \delta(\epsilon_{\mathbf{k}+\mathbf{q}})$: this term guarantees that electrons can only scatter between states that are both on the Fermi surface with energy zero, which is what Cooper demonstrated.

All of these parameters are determined by the structure of the atoms (ions and electrons) in a superconductor. It was proposed by Milan Allan and Mark Fischer [1] that holes can periodically be created in a two-dimensional superconductor to change λ . We consider now how creating holes can affect the parameters in Equation 2.6 and the effect they have on λ and therefore on T_c .

1. **Kinematic constraints:** this is the terms $\delta(\epsilon_k)$ and $N(0)$ which is the effect of electrons on the superconducting properties. These are determined by the density of states of the electrons, which determines the amount of electrons on the Fermi surface. Creating holes in a lattice will cause some ions to be removed resulting in a reduced number of orbitals being available for electrons, consequently changing the density of states.
2. **Phononic structure:** this is the phonon dispersion relation $\omega_{\mathbf{q}}$ which determines the frequency of the phonons that can cause scattering between electrons. It was shown by simulation that the effect of this on λ is minimal and can therefore be neglected [1].
3. **Electron-phonon coupling:** this is the amplitude of an electron being scattered between various states. Section 2.1.2 showed the form of the term $g(k, q)$ for a one-dimensional monoatomic chain:

$$g(k, q) = -4i\alpha \sin\left(\frac{qa}{2}\right) \cos(ka) \quad (2.7)$$

The possible wavevectors are given by

$$q, k = \frac{2\pi m}{Na} = \frac{2\pi m}{L} \quad m \in \mathbb{Z} \quad (2.8)$$

where a is the size of a unit cell and N is the number of unit cells in the chain, so $L = Na$ is the size of the chain. From this it is clear that changing the size of a unit cell by creating holes (because we increase the periodicity) will change a but will not affect the allowed wavevectors. $g(k, q)$ does contain the size of the unit cell a explicitly though, so creating holes will affect the coupling directly.

We have now looked at ways to affect the λ parameter but from mere inspection we cannot determine if the change will be positive, resulting in a higher T_c . For this we must consult the simulations [1].

2.3 Impedance and Phasors

The three most common passive electrical components are resistors, capacitors, and inductors. Consider now what the current is through each of these components when an alternating voltage is applied, with a form as given by

$$V(t) = V_0 \cos(\omega t) \quad (2.9)$$

This gives the following currents:

$$I_R(t) = \frac{V_0}{R} \cos(\omega t) \quad (2.10)$$

$$I_C(t) = -\omega CV_0 \sin(\omega t) = \omega CV_0 \cos\left(\omega t + \frac{\pi}{2}\right) \quad (2.11)$$

$$I_L(t) = \frac{V_0}{\omega L} \sin(\omega t) = \frac{V_0}{\omega L} \cos\left(\omega t - \frac{\pi}{2}\right) \quad (2.12)$$

We can write these as phasors (complex representations of physical quantities) which becomes:

$$V(t) = V_0 e^{i\omega t} \quad (2.13)$$

$$I_R(t) = \frac{V_0}{R} e^{i\omega t} \quad (2.14)$$

$$I_C(t) = \omega CV_0 e^{i(\omega t + \frac{\pi}{2})} \quad (2.15)$$

$$I_L(t) = \frac{V_0}{\omega L} e^{i(\omega t - \frac{\pi}{2})} \quad (2.16)$$

The impedance of a passive element is defined as the time-independent ratio of its complex voltage to its complex current, i.e. $Z = \frac{V(t)}{I(t)}$. For these components we find the following:

$$Z_R = R \quad (2.17)$$

$$Z_C = \frac{1}{i\omega C} \quad (2.18)$$

$$Z_L = i\omega L \quad (2.19)$$

This definition of a complex impedance allows us to define a time-independent value for AC circuits which is analogous to resistance in DC circuits. For AC circuits we can work in the frequency ω domain and simply add up series and parallel impedances in the same way as it is done with resistors. This gives an impedance in the general form $Z = |Z|e^{i\phi}$.

Consider now an arbitrary circuit of capacitors, inductors, and resistors to which we apply a sinusoidal voltage $V(t)$ and measure the sinusoidal current $I(t)$ through it. The ratio of their amplitudes gives the absolute value of the impedance and the phase difference gives the phase angle of the impedance. Using this information we can construct the complex impedance phasor, but there is no way to deconstruct this to figure out how much of this impedance comes from resistors. It would seem logical that the real part of the phasor is Z_R and the complex part to be a combination of Z_C and Z_L . Unfortunately this is not the case: we can merely calculate the total contribution due to resistors, capacitors, and inductors.

Every physically realized measurement system contains an inherent capacitance and inductance because of wires and other metal components which can store charge or have current induced in them. This puts a limitation on measurements done with AC currents because we cannot deconstruct our impedance into components, so we can never measure only the resistance of a system. An obvious solution to this problem is to measure using low frequencies or even using DC currents.

2.4 Four-terminal Resistance Measurement

It often occurs that a measurement needs to be done of the resistance of a resistor which has a very small value. This becomes problematic when the resistance of the wires or contact pads used for the measurement is larger than that of the sample, because their impact on the measurement can no longer be neglected. A simple ohmmeter which measures the resistance between two terminals consists of a voltage source in series with an ammeter as shown in Figure 2.1 below.

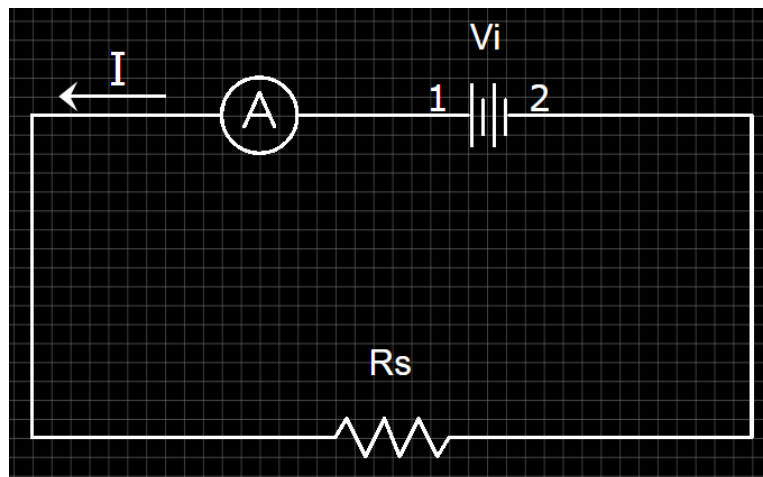


Figure 2.1: The circuit diagram for an ideal two-terminal ohmmeter. In the simplest case this is an analog galvanometer in series with a known DC voltage source such as a battery.

This is what our circuit would look like for the case of an ideal measurement. A constant voltage V_i is applied and the current I is measured using an ammeter (such as a simple analog galvanometer). The resistance can then be determined by $R_s = \frac{V_i}{I}$. A real measurement has wires (and sometimes contact pads) with a resistance of their own, leading to a mea-

sured resistance which is the sum of all of these contributions, as shown below in Figure 2.2.

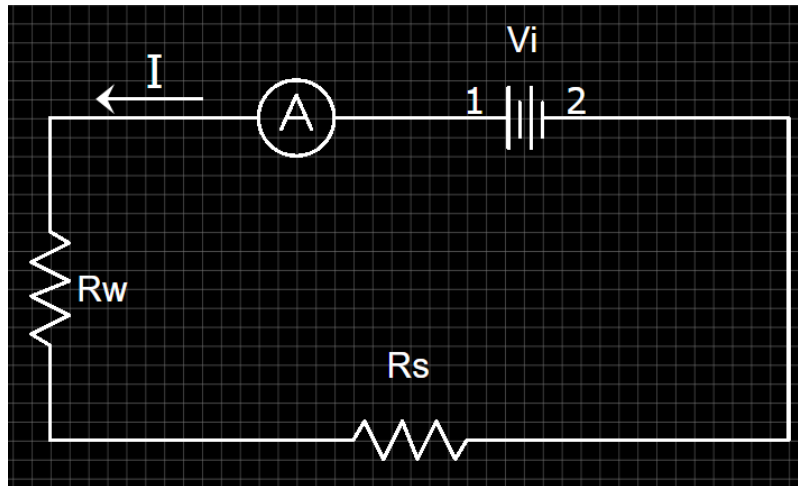


Figure 2.2: A non-ideal ohmmeter. The resistance of the wires required to perform the measurement must now be taken into consideration. For a simple ohmmeter the contribution of the wires can be removed from the total resistance by shorting the circuit, i.e. removing the sample resistor and connecting the measurement probes to determine the wire resistance. For the case that contact pads are attached to the sample this cannot be done.

For a standard resistance measurement the ohmmeter can be shorted (connecting the two measurement probes) so that the resistance of the wires is measured and is defined as zero resistance to remove the offset. If the resistance of a small sample needs to be measured via contact pads it is not possible to place the contact pads against one another, so the ohmmeter resistance cannot be measured.

To solve this problem the four-point measurement was invented. This method consists of a voltmeter placed over the sample (resistor) while simultaneously applying a large current using a current source. This works because the current through the sample will be much larger than that passing through the voltmeter due to its large internal resistance. Because of the large current passing through the sample relative to the voltmeter, the voltage drop over the wires of the voltmeter can be considered as negligible compared to the voltage over the sample. The conceptual setup can be seen below in Figure 2.3:

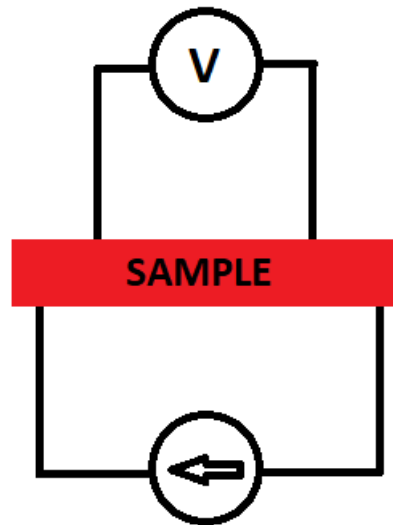


Figure 2.3: A conceptual diagram of a four-point resistance measurement. A large current source is connected to the small resistor and an external voltmeter measures the voltage over the sample.

A calculation will now be done to clarify this concept. First consider the circuit diagram of the four-point measurement in Figure 2.4. The voltmeter consists of an ammeter indicated by the letter “A” and a large internal resistor R_0 . The voltmeter is connected by wires with resistance R_2 to the sample which has resistance R_s .

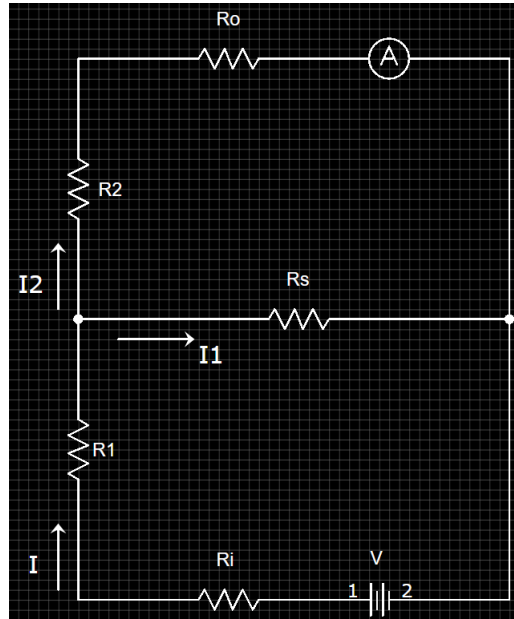


Figure 2.4: The schematic of the four-point measurement circuit. The top part is the voltmeter while the bottom part is the current source, both of which have wires with a resistance that connect to the sample.

The current source consists of a voltage source V and an internal resistance R_i connected by wires with resistance R_1 to the sample. The internal resistance of the current source is much larger than the resistance of the wires and the sample, and because the voltmeter contains a large resistor which is in parallel with the sample, its resistance as seen by the current source is negligible. In other words, the total load resistance as seen by the current source is

$$R_1 + \frac{R_s(R_2 + R_0)}{R_s + R_2 + R_0} \approx R_1 + \frac{R_s R_0}{R_0} = R_1 + R_s \ll R_i \quad (2.20)$$

Here we used the fact that $R_0 \gg R_2, R_s$. Using the relation in Equation 2.20 the supplied current becomes:

$$I = \frac{V}{R_{total}} \approx \frac{V}{R_i + R_1 + R_s} \approx \frac{V}{R_i} \quad (2.21)$$

This shows that the supplied current is largely independent of the applied resistor as long as its resistance is much smaller. For this circuit we know the values of the variables V, R_i, R_0, I, I_2 (because we either apply them or measure them) and we have the following equations:

$$V = I(R_i + R_1) + I_1 R_s \quad (2.22)$$

$$I_1 R_s = I_2 (R_2 + R_0) \quad (2.23)$$

$$I = I_1 + I_2 \quad (2.24)$$

Because the internal resistance of the voltmeter is much larger than the resistance of the wires we find the following result:

$$R_2 + R_0 \approx R_0 \quad \text{for} \quad R_0 \gg R_2 \quad (2.25)$$

Therefore we can rewrite Equation 2.23 as:

$$I_1 R_s \approx I_2 R_0 \quad (2.26)$$

Using this we also find the following relation:

$$I = I_1 + I_2 = \left(\frac{R_0}{R_2} + 1 \right) I_2 \gg I_2 \quad (2.27)$$

By applying this together with Equation 2.23 and 2.24 this becomes:

$$R_s = \frac{I_2}{I - I_2} R_0 \approx \frac{I_2}{I} R_0 = I_2 \frac{R_i R_0}{V} = R_i \frac{V_{meter}}{V} = \frac{V_{meter}}{I} \quad (2.28)$$

V_{meter} is the voltage $I_2 R_0$ as measured by the voltmeter. The sample resistance is therefore simply the voltage measured by the voltmeter divided by the current supplied by the current source. Because of the large current source the resistance of the wire R_2 has become negligible compared to the load resistance, allowing us to measure small resistances.

Experimental Procedure

Preparing a superconducting material to measure the temperature dependence of the resistance is a long process. There are many complicated steps involved, so before going into depth into each of the production techniques, a broad overview of the entire process is given here.

3.1 Outline of the Production Process

The superconductors (SC) used in this process are tiny flakes of the order of a single millimeter. This makes it difficult to work with: we can neither store it like this because it can get damaged if we pick it up nor can we mount it on a sample holder in the e-beam. Additionally, we need sufficient room around the flake to attach contact pads to the flake, allowing us to connect wires for the measurement. We therefore require a substrate on which the SC can be placed so that we can easily move it and there is enough room to create contacts. The substrate used for this is crystalline silicon. Small squares are cut from these large silicon wafers and are subsequently chemically cleaned. From now on we refer to these squares as our wafer or sample.

The next step is extracting flakes of SC of several layers thickness from the bulk material that we start with, and to get these flakes onto a silicon wafer. This process is called exfoliation. As will be explained later, to get these flakes onto the wafer we first need to clean the wafer more thoroughly and rid it of all organic material. This deep cleaning is done using an oxygen plasma, known as Reactive Ion Etching (RIE). Now several layers of SC can be removed from the bulk material and placed on the wafer. This process of exfoliation requires the use of scotch tape, so

the wafer will now be covered in glue from the tape. To remove this the sample is cleaned again with RIE.

Following this we want to create large contact pads on the wafer which are connected to the flake. These large pads are necessary because the flake is too small to attach wires to, so we attach the wires used for our measurement to these contact pads. The first step in creating these pads is to use the spin coater to distribute a layer of PMMA 950k over the wafer with the flake on it. PMMA is a plastic polymer with large chains of molecules. The 950k in the name indicates the size of the polymer chains.

The next step is to use e-beam lithography on our sample which writes a design into the PMMA using a beam of electrons. These electrons break the polymer chains so that, when placed in a chemical solution of MIBK, the broken chains dissolve, and we are left with a layer of PMMA on our sample with a pattern written into it. The first pattern that we write is a markerfield, which we write in the vicinity of a flake on our sample. In this way, we know the position of the flake on the wafer with respect to the markerfield. Next we use the e-beam again to write a design which places 4 contact pads around our flake and attaches these to the flake. This is again done by simply drawing a design in the PMMA, and then we dissolve the broken chains in MIBK again.

The contact pads design that is attached to the flake is now simply drawn in the PMMA, so we cannot attach wires yet. We now need to sputter our sample with gold. This distributes a uniform layer of gold over our entire wafer. After we do this we place our sample in a chemical bath of acetone, which breaks and dissolves all of the remaining PMMA. Because we had drawn a contact design into the PMMA earlier, these points have no PMMA remaining which could dissolve, so the gold that is there stays in its place. At the places where we did not write into the PMMA, dissolving this will cause the PMMA, which lies under the gold, to lift off, causing the gold on top of it to break off as well. The final product is a clean silicon wafer with a SC flake on it which has gold contacts attached to it.

We now attach our sample to a puck by wire bonding, which is a sample holder used by the PPMS, which is what we use to measure the resistance-temperature behavior. The puck has contact pads on it as well, which connects to the PPMS system so that currents can be passed through. We need to connect the contact pads attached to our flake to those on the puck, enabling the PPMS to measure the resistance of our superconducting material as it lowers the temperature.

3.2 Production Techniques

3.2.1 Preparing a Substrate

We start our process by preparing a substrate on which our SC can be placed. This substrate is crystalline silicon. It comes in large, thin, circular wafers which can be cut into pieces using a diamond tip pencil, called cleaving. They are cut approximately into squares of 1x1cm, but they can be no larger than that because the PPMS puck allows for up to 1x1cm samples. Cleaving becomes easier with practice, but there is a factor of luck involved that determines the quality of a wafer. Namely, a thin line is cut into the large wafer and is then broken along this line. However, crystalline silicon has a parallelogram-shaped crystal structure, so the sides often break off at an angle. A wafer with slanted sides is very difficult to pick up with tweezers and will most likely result in the sample being dropped several times. At later stages of the production process the cost of dropping a sample becomes too great, because many hours have been put into the production. We therefore want to minimize risk as much as possible, so in this beginning stage it is important to create good substrates with sides that are perpendicular to the top surface.

In order for the later stages of production to go smoothly we need to keep our sample as clean as possible throughout the process. Cutting the silicon results in a large amount of silicon particles to accumulate on the wafer as well as organic material from the surroundings. We want to remove this as much as possible. To remove the dust we blow it off with a pressurized nitrogen gun. This blows out N₂ gas which is more inert than O₂, so the gas will not react with anything on our sample. To remove organic material we place our wafer in an acetone bath for several minutes. For a deeper cleaning the beaker containing acetone and our sample can be placed in an ultrasound bath at a temperature < 50° because acetone boils above this temperature.

When acetone dries it creates stains that are very difficult to remove. For that reason we don't allow the acetone to dry on our sample. Instead we place our sample in a bath of isopropanol for a while to clean the acetone off. After this we can dry the sample using the nitrogen gun again.

3.2.2 Exfoliation and Reactive Ion Etching

Now that we have a clean wafer, we want to get flakes on it by exfoliation. The superconducting material comes in bulk pieces of approximately 1mm. We place this on a line of scotch tape and then fold the tape over on

itself. Gently rub on the bulk through the tape to improve the contact between the bulk and the tape. Now rapidly pull the tape apart, resulting in a half of the bulk on both pieces of tape. Repeat this process so that you have two pieces of tape each with around 10 sites with flakes within a region of 1x1cm.

We cannot simply pick these flakes up from the tape and place them on the wafer. Instead we place the wafer upside down on top of the flakes on the tape. Place this on a microscope slide as a stage, and heat the system at 100° for 2 minutes. The idea here is that the air in the pockets between the flakes and the wafer decreases in density because of heating. When we cool the system, the reduction in temperature causes a kind of suction which, in addition to the usual van der Waals attraction, causes the flakes to stick to the wafer.

The efficiency of this process, however, is extremely dependent on how clean our sample is. A cleaner sample results in better contact between flake and wafer, and thus stronger attraction. To achieve this higher level of cleanliness we use the Reactive Ion Etcher (RIE). This process uses an oxygen plasma to clean the wafer by reacting with organic material on the surface. Therefore we need to clean the wafer with RIE before exfoliation. The number of flakes that attach to the wafer by exfoliation is noticeably much greater after doing RIE for 10 minutes.

The process of getting flakes on the wafer by use of scotch tape results in a large amount of glue sticking to the surface of the wafer, as can be seen in Figure 3.1 below. This makes it hard to see the flakes under the optical microscope and will make it difficult to perform e-beam lithography. To remove this glue we can do RIE again for 20 minutes.

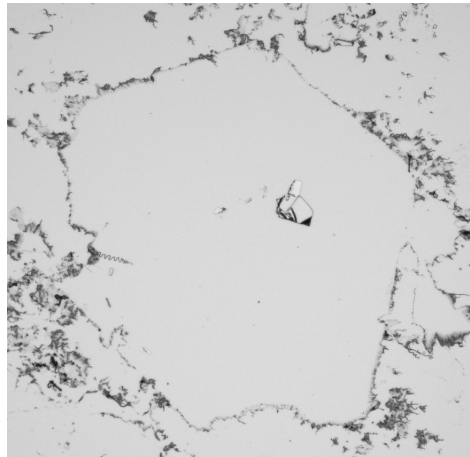


Figure 3.1: The shape of the NbSe₂ bulk material can be seen in the surrounding glue residue remaining after exfoliation. Only a small flake has stuck to the substrate. The number of flakes can be increased by cleaning the substrate more thoroughly using RIE.

3.2.3 Electron Beam Lithography (EBL)

The process of electron beam lithography (EBL) is used to write a design into a layer of PMMA which lies on our sample. The purpose of this is to either etch or sputter our sample in the shape written into the PMMA. The steps involved in the fabrication process of EBL are listed below:

1. Design: create a design (e.g. contact pads) in the EBL program
2. Expose: the design is written into the PMMA using an electron beam
3. Develop: the sample is placed in MIBK so that the broken polymer chains in the PMMA dissolve
4. Etch or sputter
5. Lift-off: remove the sputtered material everywhere except at the places where the e-beam wrote into the PMMA

To be able to write a design on our sample we first need to cover it in a layer of PMMA, a substance consisting of long polymer chains. The sample needs to be covered in PMMA 950k using the spin coater. The spin coater spins the sample at 4000rpm resulting in a single drop of PMMA to be spread out almost uniformly over the sample. Following this the resist needs to be baked at 180°C for 2 minutes by placing the sample on a hot

plate. Under the optical microscope it can be seen that the color of the PMMA is slightly different on the edges because it is a bit thicker there. The color change arises due to thin film interference of the light passing through the transparent PMMA which depends on the thickness of the PMMA.

Now we need to find a good flake on our sample that we want to measure. The layer of PMMA should make it easier to see the flakes, which are transparent with a slightly green tint, also due to thin film interference. The thickness of the flake could in practice be determined from the color of the interference, seen below in Figure 3.2. The color-thickness relation is material specific, but for NbSe_2 this information was not available.

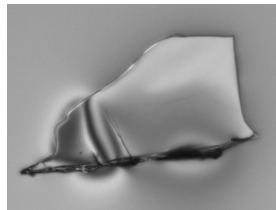


Figure 3.2: The thickness of a flake of NbSe_2 is indicated by the interference of light as it passes through a flake covered in a layer of PMMA resist. Looking through the eye piece of the microscope gives a colored image but the camera used to make images like this one is only black and white.

We are not yet going to select a specific flake. Instead it can be seen that there are regions on the wafer of about 1mm which contain many small flakes, seen below in Figure 3.3. This is because our bulk material is about 1mm in size but the exfoliation process breaks the flakes into smaller pieces within this 1mm region.

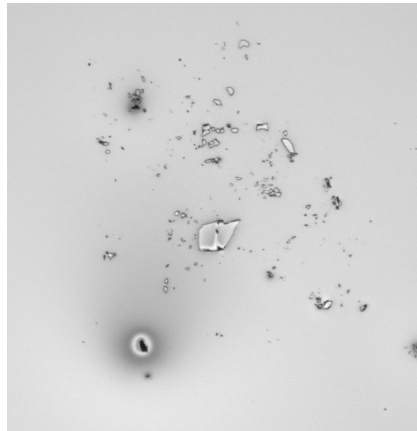


Figure 3.3: The substrate contains regions with a high density of superconducting flakes at places where the bulk material was broken into smaller pieces.

When a region with a high density of flakes has been selected we want to use the electron beam lithography system to write a markerfield over these flakes. To do this we first need to look at the sample under the optical microscope and find the coordinates of this region with respect to a corner of the wafer. We then use the e-beam to write a markerfield there. This will break the polymer chains in the PMMA so that they can dissolve in a solution of MIBK. After this process we can view our sample under the optical microscope again and see that our flakes have been divided up into spaces of a coordinate grid. If the thickness of the flakes is relevant for the process, the sample can now be looked at using Atomic Force Microscopy (AFM), which can be used to measure the thickness of the flakes. With a markerfield in place it becomes easy to know the position of each flake. This is convenient so that, when a flake has been found to be sufficiently thin by AFM, we can record its coordinates in the markerfield.

We want to select a flake of high quality. The quality of a flake is determined by several factors. Firstly the thickness needs to be considered: to investigate the two-dimensional superconducting properties of a material, the thickness must be less than the coherence length. This means that we do not have superconducting currents in the third dimension, so we can consider this system to be two-dimensional. For NbSe_2 the coherence length is somewhere between 90nm and 110nm [4]. Secondly the flake must be large enough to attach contacts to it, which means that it should be larger than $10\mu\text{m}$. In addition to this we want our flake to have a near-uniform thickness. This is important because the transition temperature is dependent on the number of molecular layers in our sample. This is relevant for samples with a small number of layers [4].

3.2.4 EBL Overlay

Once a flake has been selected in the markerfield we want to attach contact pads to it. To do this we first need to write the contact design in the PMMA again using e-beam lithography. Because we are putting this contact design over the markerfield design we call this process an overlay.

Firstly we need take a picture of the flake we want to use under the optical microscope. This picture should clearly show the flake and its coordinates in the markerfield. This image will most likely not be perfectly straight, so to fix this we use the straighten tool in the program IrfanView. This now allows us to crop the image as a perfect rectangle with local alignment marks at the corner points of the image and the flake inside. We now need to find the XY-coordinates of the corners of this image so that it can be imported into the e-beam program. These coordinates need to be placed in an .scc file containing the name of the cropped image of the flake. The .scc file can now be opened in the e-beam program making the image appear at the correct place in the markerfield, as seen in Figure 3.4 below.

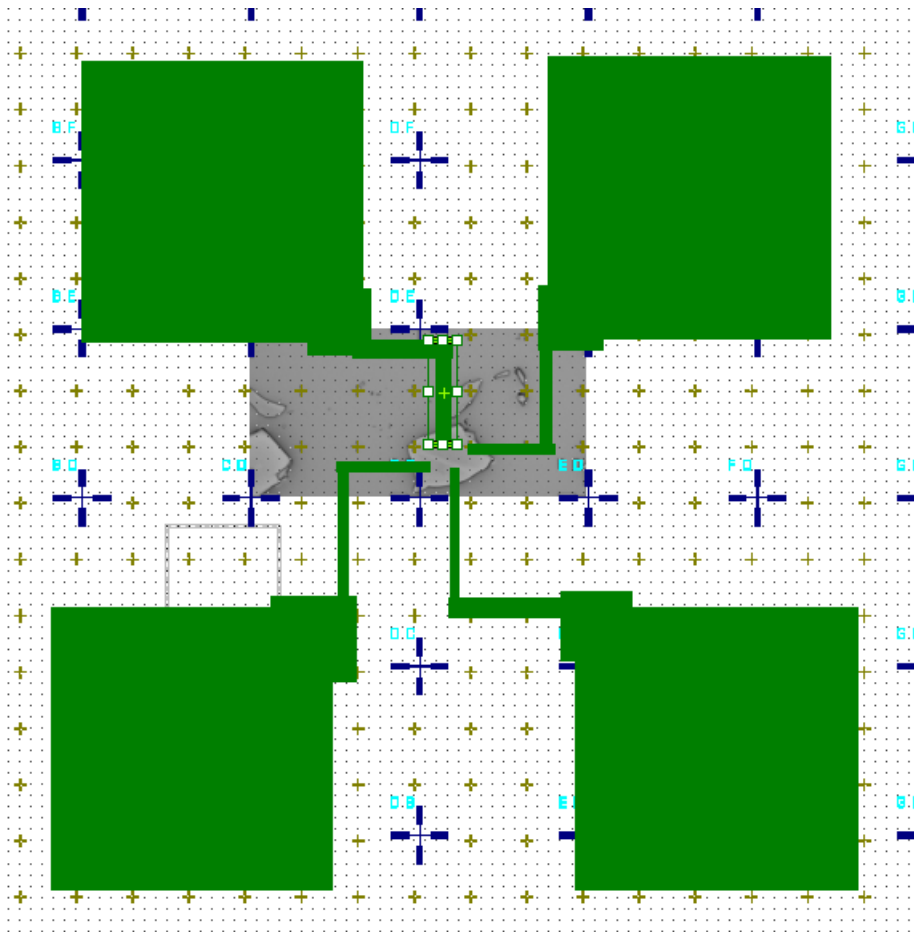


Figure 3.4: Example design for contact pads attached to a flake in a markerfield.

The next thing to do is to draw the contact pad design onto the flakes. This is done using two layers: the first layer contains the large square contact pads of size $250 \times 250 \mu\text{m}$ and the second layer contains the small contacts going from the large pads to the flake. The reason for having two different layers is that these will be written using different resolutions, known as the PC value of the e-beam. The large pads are written using PC 1 which is of low resolution but can be done quickly. The small contacts are written using PC 10, which takes longer but is more accurate. Separating these two layers also allows us to define different working areas for each layer, which gives the region over which the e-beam moves. Because the small contacts need to be precisely written we need to be careful not to make the e-beam move over a large area, because that can cause the beam to become decalibrated with respect to the sample, resulting in the contacts appearing next to the flake rather than on it. The design of these two layers

on the flake can be seen in Figure 3.4 above.

Experience teaches us that several things can ruin the design if we are not careful. Firstly we need to take the global marks into consideration that were written with the markerfield and to take care that these do not connect two contacts pads, as seen in Figure 3.5 below. If a voltage is applied to these pads a current can pass directly between the pads via a global mark - this would ruin our resistivity measurement of the flake.

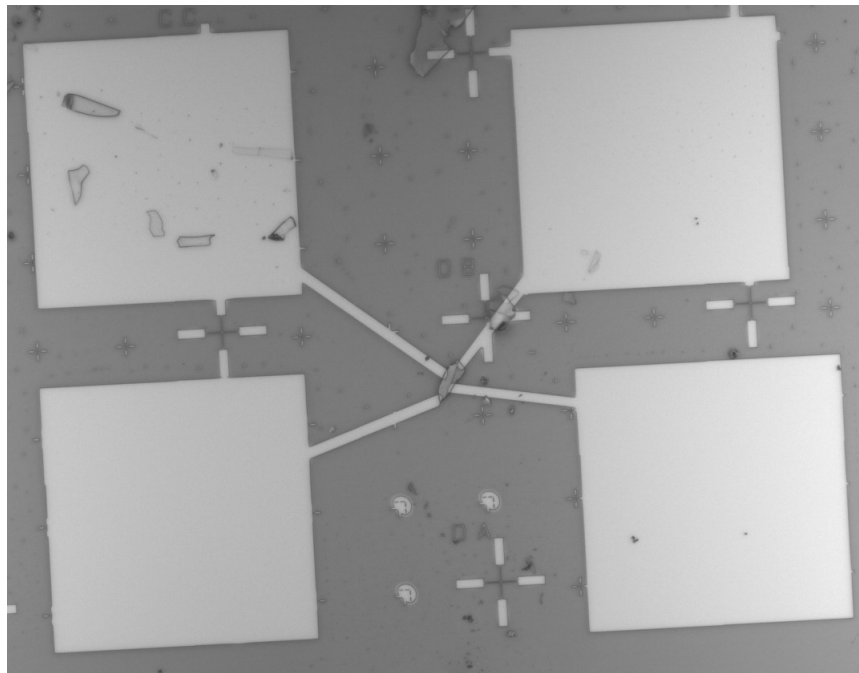


Figure 3.5: The two left contact pads are connected by a global mark causing a short circuit.

Secondly, when drawing the small contacts it is simplest to use the polygon tool as was done in Figure 3.5. Polygons, however, are arbitrarily shaped and therefore difficult for the pattern generator in the e-beam to process. It tries to break these arbitrary shapes down into fundamental triangles which requires a lot of processing power. The writing of such a complicated design could cause the system to crash resulting in a sample that looks like Figure 3.6 below, where the program crash ruined the small contacts. Instead of using polygons we need to use only rectangles, so that our design looks like Figure 3.4.

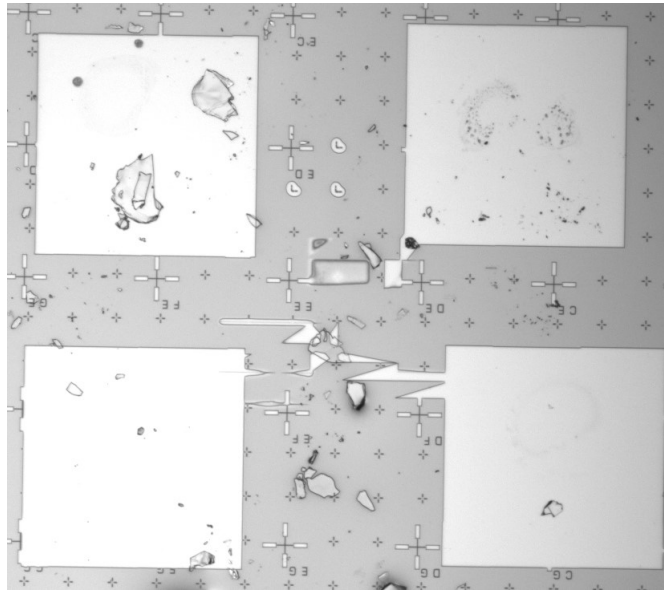


Figure 3.6: Pattern generator crash due to over-processing of polygon shapes in the design of the small contacts.

Again, when using only overlapping rectangles, care needs to be taken because it can result in Figure 3.7 where the large contact pad on the bottom left doesn't connect with the small contacts. This results from the fact that the alignment is never perfect, so enough room needs to be left for error.

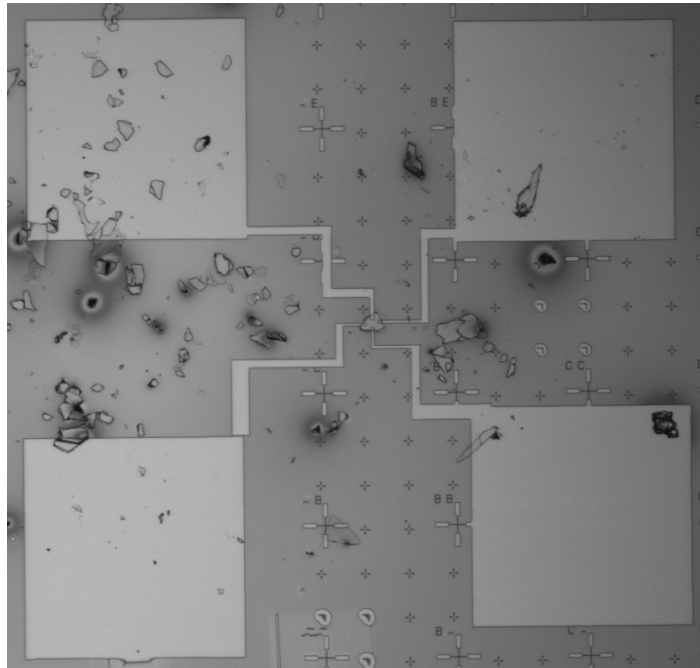


Figure 3.7: A bad alignment of the e-beam can cause gaps between contacts as can be seen on the bottom left.

As seen in Figure 3.8 below there should be a large area of overlap between the two layers so that a shift in the alignment will not cause a gap in our design. There is a large square added to the small contact layers to ensure an overlap between the large and small contact layers.

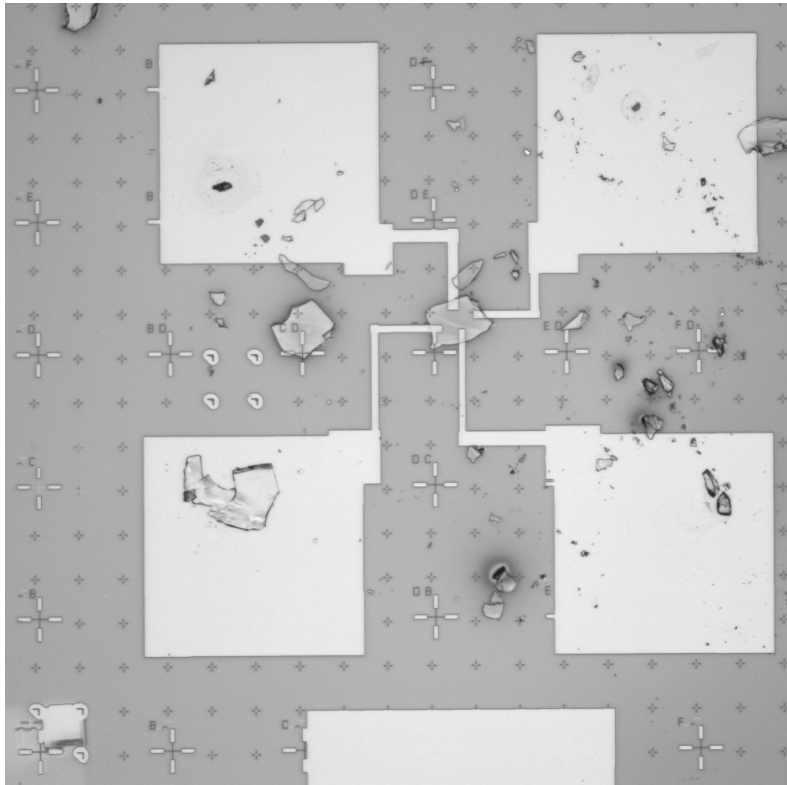


Figure 3.8: Contact pad design using only rectangles. A large square has been used to increase the area of overlap between the large pads and the small contact lines.

As has already been mentioned, to do the overlay we need to do an alignment. This entails using the crosses that are written with the markerfield (see Figure 3.4) to align our contact pads with the flake. The large crosses are called global marks which are used to compensate for a shift in our sample in the e-beam relative to its position when the markerfield was written. This change in position occurs because we put our sample in the e-beam in a slightly different position every time, and each time it could be slightly rotated. The global mark alignment compensates for this. The smaller marks, called local marks, are used to calibrate the electron beam. This calibration is called a writefield alignment which ensures that the electron beam can accurately write each piece of our design which lies in each writefield. A writefield is the region over which the electron beam can tilt. Therefore the total design is written by shifting the stage on which our sample lies by one writefield, and then writing the part of the design inside this writefield, and then moving the stage to the next writefield.

3.2.5 Sputtering and Lift-off

Now that we have written a design for our contacts into the layer of resist using EBL, we want to turn these shapes into gold contacts. This goes according to the process shown in Figure 3.9 below. We see that after lithography we need to sputter our material. To do this the sample needs to be placed in a sputtering chamber which is subsequently pumped down to near-vacuum. At the top of the chamber is the target which is a plate containing the material that we would like to cover our sample with, such as gold. Argon gas is injected into the system and it is turned into a plasma by an oscillating electric field. A potential difference is applied to the target so that the particles in the argon plasma are accelerated towards the target, colliding with the material, resulting in particles of the target being sprayed isotropically in the chamber. This results in a uniform layer of sputtered material on our sample.

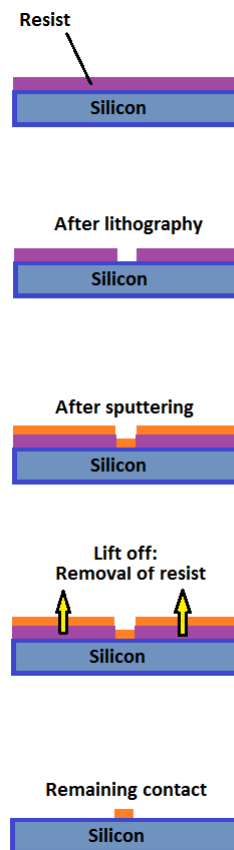


Figure 3.9: The sputtering process.

At the places where the design was written with the e-beam, the resist has been removed. At those points the sputtered gold is directly touching the substrate. At the points where there is still resist, the gold lies on top of the resist. If the sample is placed in an acetone bath the resist will completely dissolve resulting in the gold that lies on top of this resist to break off. This removal of resist and the attached gold is called a lift-off. The lift-off may not work completely by only dissolving in acetone because the sputtered gold may be difficult to remove: it has also filled all the valleys in the resist created by the markerfield. To initiate the lift-off process it may be necessary to gently rub along the edge of the substrate with a cotton swab to break off the gold. This creates an opening through which the acetone can enter beneath the layer of gold.

Another way to accelerate the lift-off is to place the acetone containing the sample in an ultrasound bath. The ultrasound should be set to a low setting of 50% to prevent the flake from being shaken loose. In most cases placing the sample in the ultrasound at 50% for about 30 seconds should be sufficient. Occasionally some stubborn pieces of gold may remain, in which case the intensity can be turned up to 75% for a few seconds. The difficulty of the lift-off can be seen in Figure 3.10 below where a lot of gold remains.

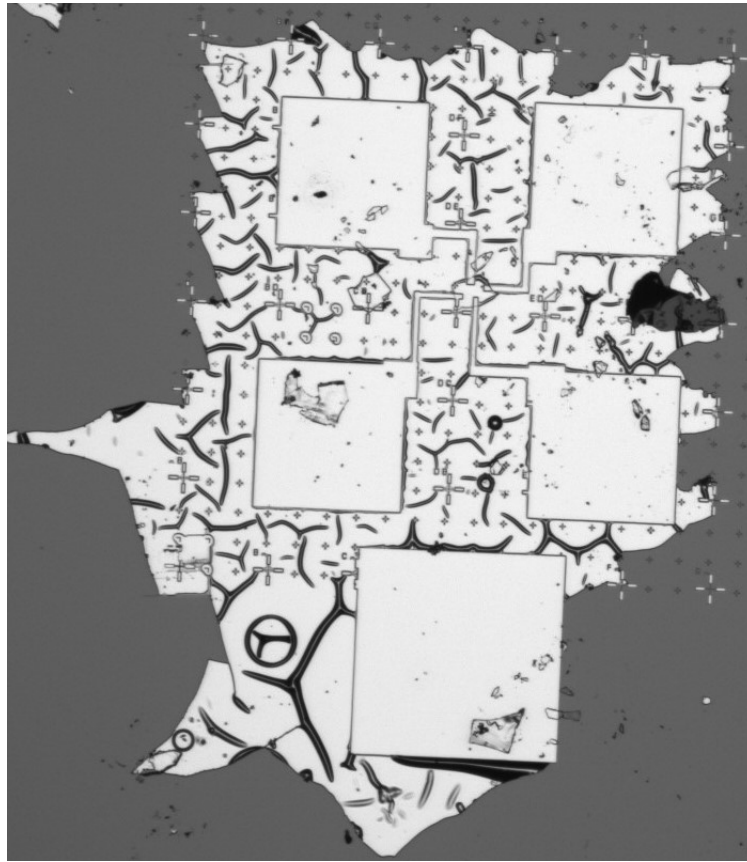


Figure 3.10: An incomplete lift-off of sputtered Au with MoGe used as a binding layer.

Sputtering gold directly onto silicon will not work well, however, because gold does not adhere to silicon. A binding layer between these two is required. For gold and silicon we can use MoGe as a binding agent. This means that we need to sputter twice: first we sputter about 5.2nm of MoGe and following this about 96nm of Au on top for a total thickness of 101.2nm.

3.2.6 Wire Bonding

In order to conduct a resistance measurement of a microscopic sample, wires need to be connected to it. Due to the small size of the sample the effective area is increased by attaching contact pads by electron beam lithography, making it easier to connect wires to this larger area. The resistance measurement is done in a Physical Property Measurement System (PPMS) into which the sample is loaded by mounting it onto a puck - a device

containing terminals which directly connect the sample to the PPMS. The sample is stuck to the puck using a small amount of silver paint. An image of the sample connected by aluminum wires from its contact pads to a puck is shown below in Figure 3.11.

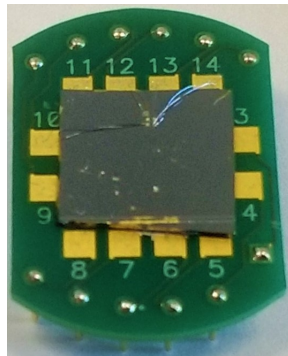


Figure 3.11: Contact pads attached to NbSe_2 flakes wirebonded to a PPMS puck.

The contact pads are $250 \times 250 \mu\text{m}$, making them only just visible to the naked eye. To accurately connect wires a microscope is required. The wire bonder has a built in microscope and is capable of connecting different materials by an aluminum wire. This is done by a process called wedge bonding which makes use of ultrasonic power to create bonds on different materials. The power, force and bonding time need to be adjusted for each material - smooth surfaces require larger values because it is harder to bond.

The following parameters are to be chosen to get the most secure bond as possible. The first four need to be chosen for both materials between which to bond; the remaining are for the overall bond:

1. Search: this determines the height from the surface to which the wedge (tip of the bonding needle) goes as you search for the correct location to create the bond. This height should be about 3 times the thickness of the wire to be bonded. When the bond is being made the tip goes from the search height down to the surface of the material to create contact.
2. Power: this sets the ultrasonic power which corresponds to the vibration frequency of the wedge.
3. Force: this is the amplitude of vibration of the wedge.
4. Time: the amount of time during which the wedge pushes the wire onto the sample during the ultrasonic vibration.

5. Loop: the length of the bonded loop. This determines the size of the arc (height) that the wire makes.
6. Tail: the amount of residual wire that is left hanging on the side of the bond.

The loop and tail should be chosen in such a way that the wire from one bond doesn't lie on another contact pad since this will create a short circuit. It is not trivial to determine whether a bond is done correctly. The connection may appear secure but a measurement of the current could imply otherwise. To improve the probability of attaining a successful connection a double bond can be made so that there are two parallel wires. This can be seen in Figure 3.12 below.

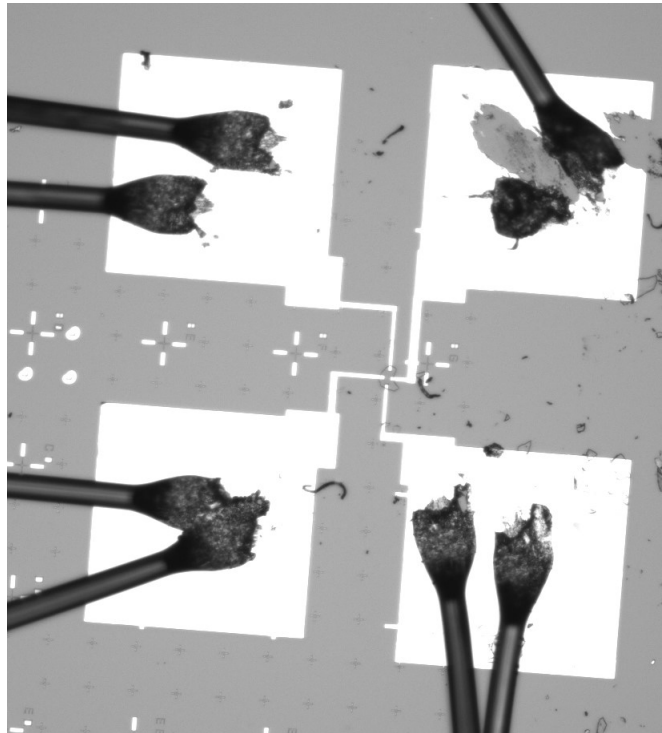


Figure 3.12: Double wires bonded between the contact pads and the PPMS puck to increase the probability of having a good connection. A bond broke off the top right pad and it can be seen that pieces of gold have broken off with it. The contact pads must therefore be made large enough so that multiple attempts or bonds can be made.

To determine the right parameters many practice bonds must be made. If the parameters are far off from their optimal value it is very common

that the wire will simply not bond to the surface. If the parameters are set too high the wire could be bonded to the surface but consequently break off, causing some of the sputtered gold on the surface to come off as well. This makes it impossible to bond on that same position again. For this reason the contact pads need to be made large enough for approximately 4 bonds. In Figure 3.12 above it can be seen on the upper right pad that pieces of gold have broken off the contact pad.

A way to work around the issue of failed or broken bonds is to add a practice pad in the overlay lithography process on which to test the wire bond parameters. As seen in Figure 3.13 below this pad can be made large and be written near the sample.

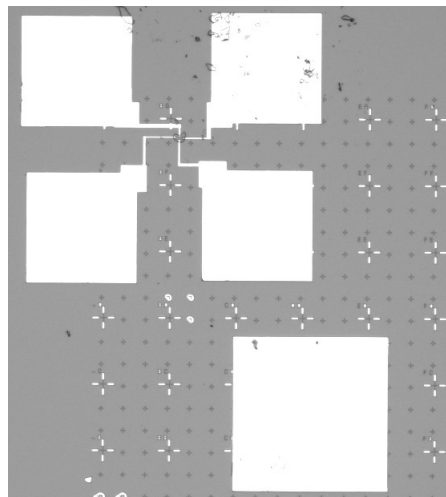


Figure 3.13: A large practice pad can be added to the e-beam design on which the wire bond parameters can be tested without ruining the valuable contact pads.

3.2.7 PPMS

To do a cryogenic resistance measurement of a sample we need to use a Physical Properties Measurement System (PPMS). This system consists of a large cryogenic tank containing an inner lining of liquid helium and an outer lining of liquid nitrogen. With these two substances the chamber can be cooled down to 2K. To place a sample in the chamber it must first be wire bonded to a PPMS puck as shown in Figure 3.11. The puck is then mounted on a rotating stage: a long rod which is subsequently placed inside the cryogenic tank.

The resistance is determined by a four-point measurement, a method that is explained in the theory section. This measurement allows for ac-

curate measurements of small resistances independent of the size of the connected wires or contact pad resistances, as long as they are all much less than the internal resistance of the voltmeter. The four-point measurement also ensures that the properties of the contact pads can be ignored. For example, the fact that there are flakes of NbSe₂ under some of the pads or that our pads are made of Au and MoGe (which is a superconducting substance) doesn't matter, because only the sample resistance is measured.

The measurement is done using a lock-in amplifier which can measure AC currents accurately even if they contain a large amount of noise. The system uses an amplifier to increase the signal size and subsequently passes the signal through several filters to retrieve a clearer signal.

To ensure that superconductivity does not break down, the value of the current source in the four-point measurement must be chosen to be less than the critical current of the sample. The critical current density is a material-specific property, which for NbSe₂ is on the order of 10^4 A/m² [5]. To get the critical current this value must be multiplied by the cross-sectional area, i.e. width times thickness. As can be seen in the results section of this thesis, the thickness was determined to be on the order of 100nm while the flake width is approximately $10\mu\text{m}$, which gives a critical current of the order of 10^{-8} A. To be safe the current should therefore be set around 1nA.

Because a measurement has many charged components, such as current carrying wires, charge can build up between various components resulting in a capacitance. This is an undesired effect in a resistance measurement because we get the total impedance of the system rather than solely the resistance of our sample. A resistor has a phase shift of zero by definition. This means that if a non-zero phase is measured in our circuit it will imply that other passive components are present, such as capacitors or inductors. These are naturally present in every real world non-ideal circuit because of the presence of wires which can act as capacitors and have an inductance. The problem with this is that the measured impedance will be the total impedance of the circuit, including that of the capacitance of the wires for example. The four-point measurement will not remove this contribution because the capacitance of a wire gives an impedance which is in parallel with the sample resistance rather than in series.

A possible solution to this is to perform the measurement using DC currents only so that the frequency is zero which removes all non-resistive impedances. It is recommended to avoid this, however, because the internal hardware of the PPMS is the AC lock-in. This is easy to use and the lock-in can remove signal noise very well so it is preferable to simply do an AC measurement at low frequencies. A measurement is only considered

reliable if the phase is less than 10° which implies that the capacitance in the circuit is small: this is the case for most systems.

Results

4.1 PPMS Measurement of NbSe₂

4.1.1 Resistance-Temperature Measurement

Once the production process has been carried out a measurement can be conducted. This is a measurement of the resistance of the superconductor as the temperature is lowered. To measure the resistance of a sample we do a four-point measurement using the AC lock-in in the PPMS, where we measure the voltage as a function of the applied current. However, as explained in Section 2.3, any AC measurement leads to contributions to the impedance due to non-resistive passive components. We therefore measure the impedance of the system including any capacitors that are in parallel with the sample resistor because these are not filtered out by the four-point measurement.

The measured results for the amplitude of the impedance of the NbSe₂ flake are shown below in Figure 4.1. The measured impedance only goes up to 1100Ω because of the sensitivity of PPMS. Therefore there is no information for the value of the impedance below about 150K, but we can be sure that it is definitely above the maximum value of 1100Ω. The plot also shows the resistance of NbSe₂ we would expect to measure at each temperature as it has been done in the past [6].

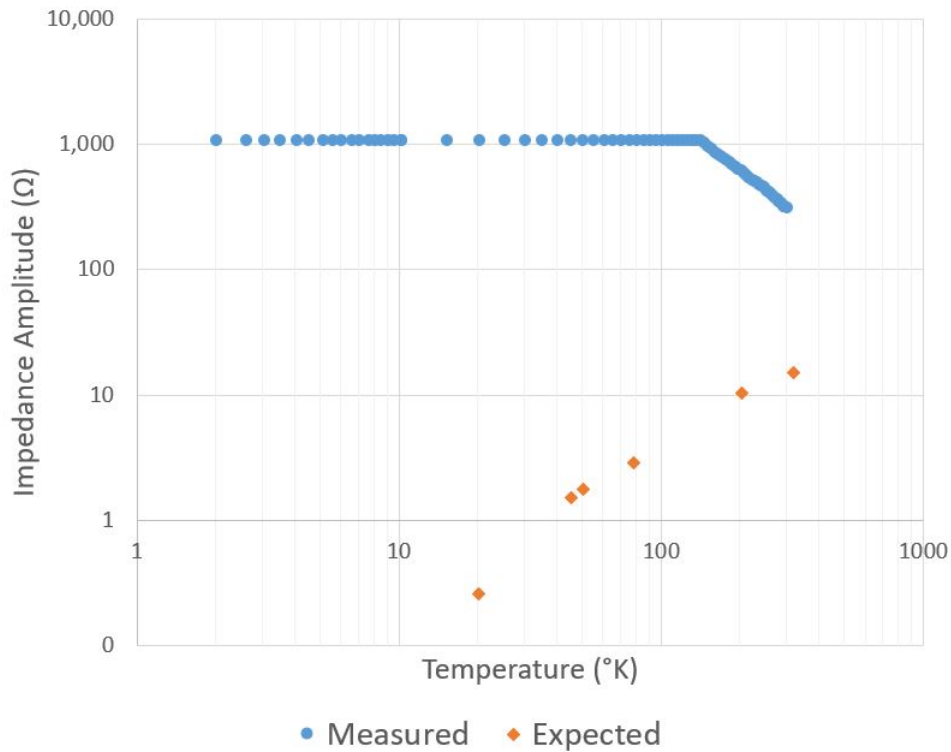


Figure 4.1: Plot of the amplitude of the impedance of NbSe₂ measured as the temperature is reduced from 300K to 2K. This is compared with the R-T curves that would be expected for the case that NbSe₂ is superconducting as compared with past measurements [6]. Due to the sensitivity setting of the PPMS the impedance peaks at 1100Ω which means that the impedance at those points is larger than 1100Ω.

The source of the expected data [6] gave measurements of the resistivity at several temperatures for a sample of NbSe₂. To go from resistivity to resistance we apply the following formula:

$$R = \rho \frac{l}{A} \quad (4.1)$$

If we assume that our flake has equal width and length of size L and thickness d we find that $A = Ld$ and therefore

$$R = \rho \frac{L}{Ld} = \frac{\rho}{d} \quad (4.2)$$

The resistance is therefore determined by the resistivity and the thickness alone. As can be seen in the next section, a flake thickness measurement

was conducted which gave a value of approximately 92nm. Using this thickness and the resistivity as given by [6] we attain the plot as seen in Figure 4.1.

The behaviour shown in this plot is completely unexpected and cannot correctly be explained. Firstly the impedance at 300K is larger than expected by about two orders of magnitude: the measured value is 320Ω and the expected value is 15Ω . This could possibly be explained if the expected data from our source [6] is incorrect; a second source of NbSe₂ resistivity values could not be found to verify this. It seems more likely, however, that our measurement was done incorrectly when we consider the second problem: the impedance appears to increase with decreasing temperature. This R-T behaviour cannot be related to any known material in nature. Generally the resistance decreases with temperature because the amount of thermal noise decreases due to a reduction in fluctuations of the current. Also for such a small sample it seems likely that the resistance at 300K would be nearer to 10Ω than 300Ω .

A possible explanation for this peculiar data is that the increasing resistance arises because the NbSe₂ flakes decrease in size as the temperature is lowered resulting in a gap between the flake and the contacts. There could still be a tunnel current when the gap is small, but this decays exponentially with gap size. As seen below in Figure 4.2 when we consider only the data below the resistance limit at 1100Ω , it appears as though the data could have a very weak exponential decay. Although the large R-squared value indicates that this is a good fit, this idea is quite far-fetched because the exponential is quite small and a linear fit also gives a relatively large R-squared value. The idea behind the exponential fit is that we assume the NbSe₂ flake reduces in size linearly with the temperature so that the resistance decreases exponentially with temperature.

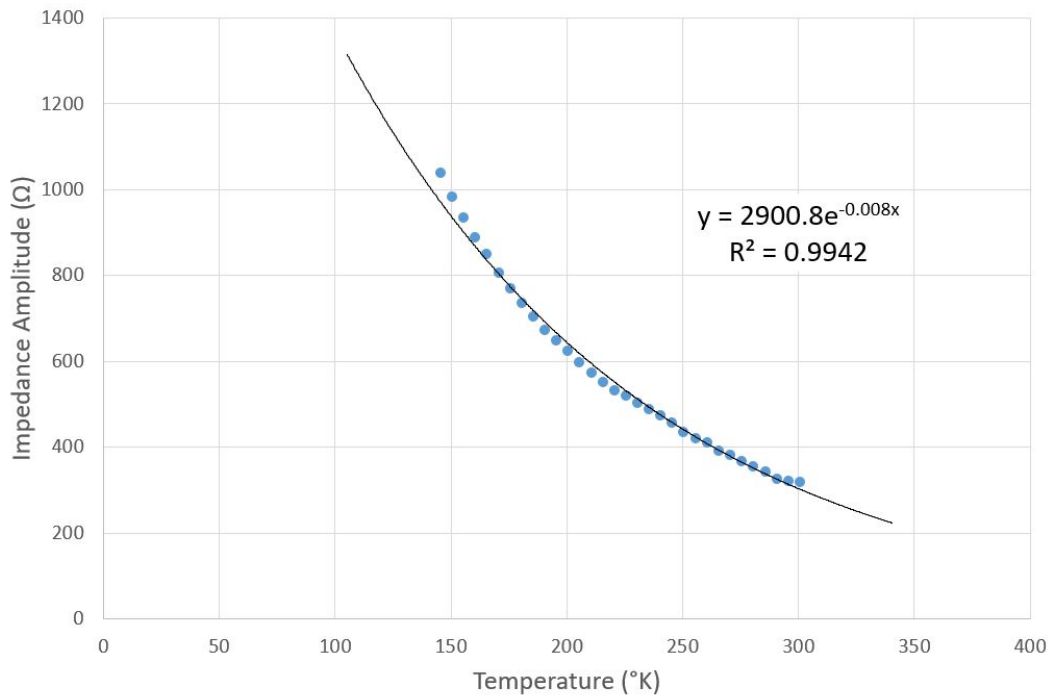


Figure 4.2: A closer look at the portion of the measured data from Figure 4.1 which decays. The data has been fitted with an exponential decay. Although the R-squared value is large, a linear fit also gives a good fit which indicates that this data is not sufficient to determine a proper relation.

This explanation could be fallible, however, because it is also possible that the contact pads adhere to the flake and therefore bend in the direction of the flake as it decreases in size. In that case there would not be gap between the flake and the contacts. There are many other possible explanations for this behaviour but until we test the limits of the measurement further by measuring more samples these statements are all merely conjecture.

4.1.2 Phase Measurement

The impedance behaviour doesn't appear to be the behaviour of a resistor so we take a look at the contribution due to capacitors and inductors. To further investigate this we take a look at the phase as a function of temperature. Because the measurement gives the total impedance of the system it is possible that the strange observed behavior is due to the change in capacitance or inductance as a function of temperature rather than the resistance. For example, it may be that the resistance of the NbSe₂ sam-

ple does decrease with temperature but the capacitor impedance increases more significantly, so we observe the dominating behaviour of the capacitor. The dependence of phase on temperature is shown below in Figure 4.3.

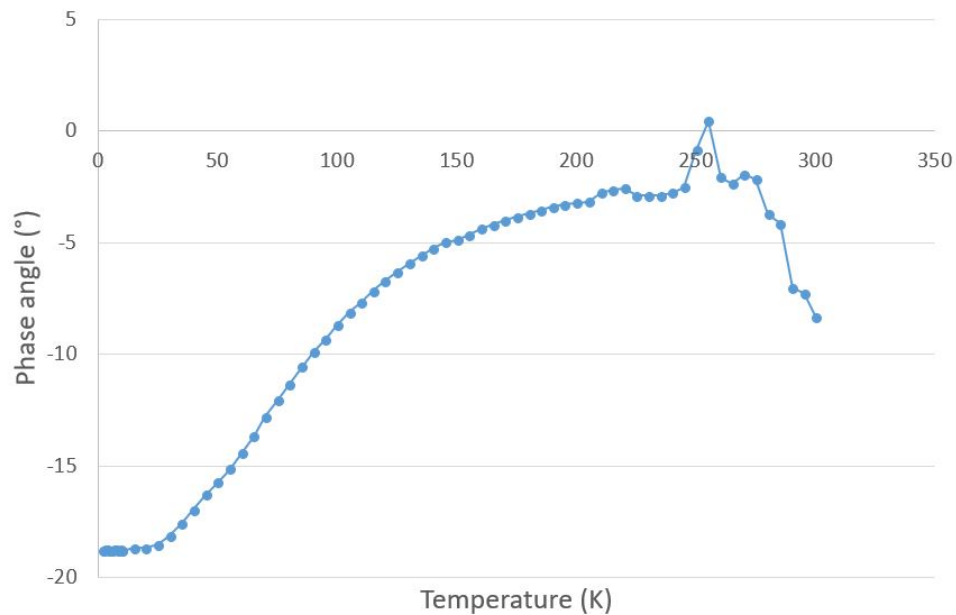


Figure 4.3: Plot of the phase angle of the impedance of NbSe_2 measured as the temperature is reduced from 300K to 2K. The phase goes further away from zero as the temperature is lowered which implies that the capacitance or inductance is increasing.

This plot shows us that the phase angle of the impedance increases (the value goes further away from zero phase) as the temperature is lowered. Unfortunately we cannot conclude that the capacitor impedance is increasing because the phase angle gives the relative phase of the signals in the circuit. We do know, however, that the four-point measurement removes impedance that is in series with our sample. Generally the impedance of wires can be modelled as an inductor in series with our sample and the capacitance of the wires will be parallel to the sample. Therefore the impedance of the inductor will be removed by the measurement and the total impedance will be a capacitor in parallel with the sample. For a parallel system the phase shift is $\tan \phi = \omega RC$ so the increasing phase can be due to either an increasing resistance or capacitance. In most systems the capacitance doesn't depend heavily on temperature, so the most likely explanation is that the resistance is increasing (assuming our grossly over-

simplified model). The cause of this is still unclear, however.

4.2 Flake Thickness Measurement

To consider all possible causes of the unexpected measurement results, aside from the measurement process, we must also take the sample into consideration. Some materials degrade over time, for example by oxidation, resulting in a change in its characteristic properties. The NbSe₂ bulk material used in this project, however, was relatively new. It is highly unlikely that it has degraded in such a short time.

Another problem to consider is that the NbSe₂ flakes are simply too thin. This could cause them to be damaged either by the exfoliation process itself or by another process, such as RIE or sputtering, both of which accelerate particles towards the sample. If the flakes are only a few layers thick they could get damaged by these processes, causing them to break or contain holes. Alternatively it is possible that, if the flakes are less than 5 molecular layers thick, their critical temperature will be below 2K [7]. This is outside of the range of the PPMS and therefore a superconducting phase transition cannot be detected. This would explain why the resistance does not go to zero, but it would not clarify the increase in resistance as the temperature goes down.

To investigate this problem the thickness of the flake was measured using the profilometer. The profilometer is not very accurate but it gives a rough idea of the thickness as seen below in Figure 4.4. There is an initial bump of approximate thickness of 95nm (because 1Å= 0.1nm) which is the thickness of the contact pad which is about 100nm. After this there is another bump which is a small contact wire and then another bump on top of that which indicates the contact wire that lies on top of the flake. Using the difference calculator in the profilometer program to subtract the thickness of the contacts from this total value the thickness was found to be 92nm.

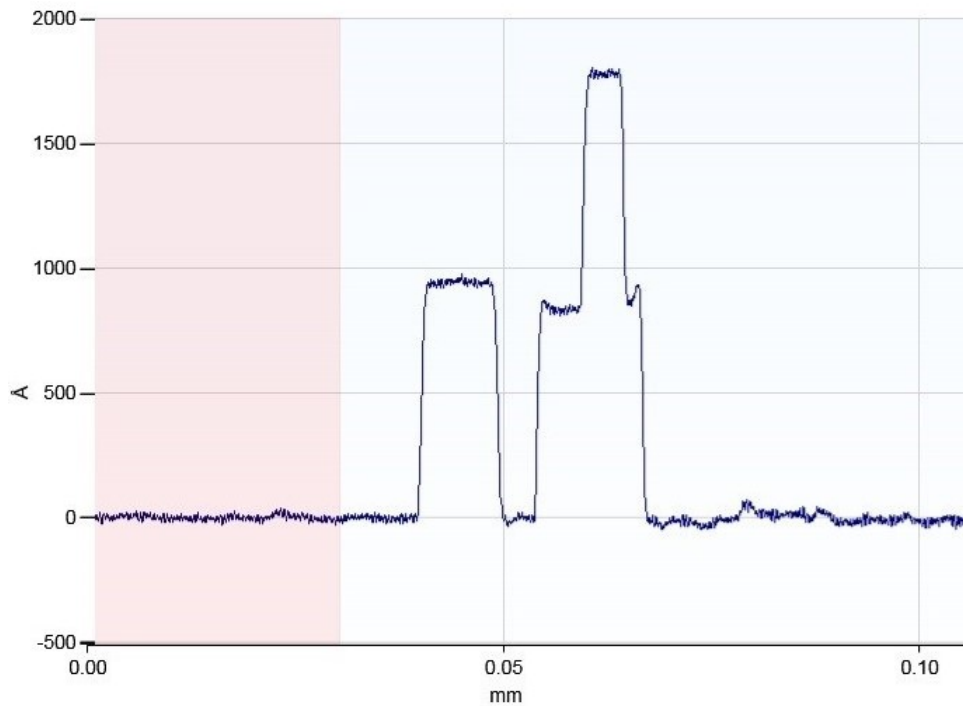


Figure 4.4: Measurement of the thickness of an NbSe_2 flake using a profilometer. The first and second bumps are contact pads. The largest bump is the thickness of a contact wire on top of the flake, so the difference between this and the first bump gives the flake thickness.

From this we can conclude that the sample is not the problem. It is not old enough to be degraded and it is too thick to be damaged by the production process. The thickness of a single layer of NbSe_2 is 0.4nm [5] so 92nm corresponds to about 230 layers. In addition to this we note that we might not be able to consider this flake to be two-dimensional. It was found that the coherence length of NbSe_2 is somewhere between 90nm and 110nm [4] while this flake lies in that range. Therefore there is a possibility that there are superconducting currents in the third dimension. To prevent this in the future Atomic Force Microscopy can be used to determine the thickness of the flakes before attaching contact pads.

Conclusion: Outlook and Further Research

Initially the purpose of this project was to explore the effect of periodic nanopatterning on the critical temperature of superconductors. In the end this turned out to be too ambitious: the time required to learn all of the steps in the measurement process was underestimated. This is firstly due to the fact that there are many steps that need to be mastered and time needs to be put in to gain experience. To make these steps easier for a successor most of the problems to watch out for have been mentioned in this thesis and possible alternatives are given. Secondly there was a maximum speed of the project which was determined by how frequently the lab technicians were available to give instructions for the different machines that need to be learned, as well as a limit on the availability of resources. The e-beam, for example, was regularly reserved, so time in the clean room needed to be planned ahead of time.

In the end holes were never made in a superconductor. This was because the measurement process was not successful. These problems can depend on numerous factors but it can be narrowed down if more measurements are done. It is possible, however, as is often the case in practical work, that we will never know what the problem was and that it was simply due to a bad connection between two components or conversely that there is a short circuit somewhere in the measurement. These can be random errors that generally cannot be avoided or the likelihood could be reduced by optimizing the measurement process. But once again, we cannot optimize until we have diagnosed what the problem is by repeated measurement.

Appendix

6.1 Diagonalization of the BLF Hamiltonian

The calculation for diagonalizing the BLF Hamiltonian is rather extensive and is demonstrated here. The calculation has insightful results and is therefore included. For the electron part the calculation is done in three dimensions while the phonon and coupling parts are more complex and so are demonstrated in one dimension only.

Electron part

Consider a three-dimensional lattice of size $N_x N_y N_z$ with lattice constants a_x, a_y, a_z . If we assume the hopping term to be equal between all adjacent atoms, the electron part expressed in three dimensional real-space coordinates is as follows:

$$H_{el} = -t \sum_{\langle \mathbf{r}, \mathbf{r}' \rangle} \left(c_{\mathbf{r}'}^\dagger c_{\mathbf{r}} + c_{\mathbf{r}}^\dagger c_{\mathbf{r}'} \right) \quad (6.1)$$

The sum is over adjacent lattice points which are separated by a lattice vector, so $\mathbf{r}' = \mathbf{r} + \mathbf{R}$ where \mathbf{r} are the lattice points and \mathbf{R} are adjacent lattice vectors, resulting in the following:

$$H_{el} = -t \sum_{\mathbf{r}} \sum_{\mathbf{R}} c_{\mathbf{r}+\mathbf{R}}^\dagger c_{\mathbf{r}} \quad (6.2)$$

Define a coordinate transformation to k-space:

$$c_{\mathbf{r}} = \frac{1}{\sqrt{N_x N_y N_z}} \sum_{\mathbf{k}} c_{\mathbf{k}} e^{i\mathbf{k} \cdot \mathbf{r}} \quad (6.3)$$

$$c_{\mathbf{r}}^\dagger = \frac{1}{\sqrt{N_x N_y N_z}} \sum_{\mathbf{k}} c_{\mathbf{k}}^\dagger e^{-i\mathbf{k} \cdot \mathbf{r}} \quad (6.4)$$

Plugging this into Equation 6.1 we get:

$$H_{el} = -\frac{t}{N_x N_y N_z} \sum_{\mathbf{R}} \sum_{\mathbf{k}, \mathbf{k}'} c_{\mathbf{k}'}^\dagger c_{\mathbf{k}} e^{-i\mathbf{k}' \cdot \mathbf{R}} \left(\sum_{\mathbf{r}} e^{-i(\mathbf{k}' - \mathbf{k}) \cdot \mathbf{r}} \right) \quad (6.5)$$

Because we have a finite lattice of size $N_x N_y N_z$ the allowed wavevectors \mathbf{k} will be determined by setting Born-von Karman boundary conditions, i.e. periodic boundaries. The lattice vectors and wavevectors for our lattice are

$$\mathbf{r} = (n_x a_x, n_y a_y, n_z a_z) \quad (6.6)$$

$$\mathbf{k} = 2\pi \left(\frac{m_x}{N_x a_x}, \frac{m_y}{N_y a_y}, \frac{m_z}{N_z a_z} \right) \quad (6.7)$$

For the values

$$n_x, m_x = 0, 1, \dots, N_x - 1 \quad (6.8)$$

$$n_y, m_y = 0, 1, \dots, N_y - 1 \quad (6.9)$$

$$n_z, m_z = 0, 1, \dots, N_z - 1 \quad (6.10)$$

Using this we can rewrite the last part of Equation 6.5:

$$\sum_{\mathbf{r}} e^{-i(\mathbf{k}' - \mathbf{k}) \cdot \mathbf{r}} = \left(\sum_{n_x} e^{-2\pi i \frac{m'_x - m_x}{N_x a_x} n_x a_x} \right) \left(\sum_{n_y} \dots \right) \left(\sum_{n_z} \dots \right) \quad (6.11)$$

The dots indicate that the argument of the n_x sum is repeated for y and z analogously. Consider now the geometric series:

$$\sum_{i=0}^{N-1} r^i = \frac{1 - r^N}{1 - r} \quad (6.12)$$

Writing Equation 6.11 in a similar form we find

$$\sum_{n_x=0}^{N_x-1} \left(e^{-2\pi i \frac{m'_x - m_x}{N_x}} \right)^{n_x} = \frac{1 - e^{-2\pi i (m'_x - m_x)}}{1 - e^{-2\pi i \frac{m'_x - m_x}{N_x}}} \quad (6.13)$$

If $m'_x - m_x \neq 0$ then the numerator is equal to zero because the difference will be an integer. The denominator is not zero because $(m'_x - m_x)/N_x$ can never be an integer since m'_x and m_x are less than N_x . In this case the sum will be zero. If $m'_x - m_x = 0$ we get an indeterminate form of type $\frac{0}{0}$ so we use L'Hopital's rule to determine the limit:

$$\lim_{(m'_x - m_x) \rightarrow 0} \frac{1 - e^{-2\pi i(m'_x - m_x)}}{1 - e^{-2\pi i \frac{m'_x - m_x}{N_x}}} = \lim_{(m'_x - m_x) \rightarrow 0} \frac{e^{-2\pi i(m'_x - m_x)}}{\frac{1}{N_x} e^{-2\pi i \frac{m'_x - m_x}{N_x}}} = N_x \quad (6.14)$$

Therefore we find

$$\sum_{n_x=0}^{N_x-1} \left(e^{-2\pi i \frac{m'_x - m_x}{N_x}} \right)^{n_x} = N_x \delta_{m'_x, m_x} \quad (6.15)$$

And so Equation 6.11 becomes

$$\sum_{\mathbf{r}} e^{-i(\mathbf{k}' - \mathbf{k}) \cdot \mathbf{r}} = N_x N_y N_z \delta_{\mathbf{k}, \mathbf{k}'} \quad (6.16)$$

This simplifies Equation 6.5 to:

$$H_{el} = -t \sum_{\mathbf{k}} c_{\mathbf{k}}^{\dagger} c_{\mathbf{k}} \sum_{\mathbf{R}} e^{-i\mathbf{k} \cdot \mathbf{R}} \quad (6.17)$$

The lattice vector \mathbf{R} can assume the following values:

$$\mathbf{R} = \pm a_x \hat{x} \pm a_y \hat{y} \pm a_z \hat{z} \quad (6.18)$$

Using this we get

$$\sum_{\mathbf{R}} e^{-i\mathbf{k} \cdot \mathbf{R}} = 2(\cos k_x a_x + \cos k_y a_y + \cos k_z a_z) \quad (6.19)$$

The electron Hamiltonian has now be diagonalized and is given as a sum over k-space:

$$H_{el} = -2t \sum_{\mathbf{k}} (\cos k_x a_x + \cos k_y a_y + \cos k_z a_z) c_{\mathbf{k}}^{\dagger} c_{\mathbf{k}} \quad (6.20)$$

Which can also be written as

$$H_{el} = \sum_{\mathbf{k}} \epsilon_{\mathbf{k}} c_{\mathbf{k}}^{\dagger} c_{\mathbf{k}} \quad (6.21)$$

From which we see that the energy of an electron with wavevector \mathbf{k} is given by

$$\epsilon_{\mathbf{k}} = -2t (\cos k_x a_x + \cos k_y a_y + \cos k_z a_z) \quad (6.22)$$

Phonon part

We consider now a one-dimensional chain of N atoms with lattice constant a because this significantly simplifies the calculation. The same diagonalization will be done for the Hamiltonian of the phonons, given by

$$H_{ph} = \sum_n \left[\frac{p_n^2}{2m} + \frac{\kappa}{2} (u_n - u_{n+1})^2 \right] \quad (6.23)$$

To transform to k -space we use the discrete Fourier transforms

$$u_n = \frac{1}{\sqrt{N}} \sum_k u_k e^{ikx_n} \quad (6.24)$$

$$p_n = \frac{1}{\sqrt{N}} \sum_k p_k e^{ikx_n} \quad (6.25)$$

where the real and reciprocal space coordinates are given by

$$x_n = na \quad (6.26)$$

$$k = \frac{2\pi m}{a} \quad (6.27)$$

For the values

$$n, m = 0, 1, \dots, N-1 \quad (6.28)$$

Now apply the Fourier transform to diagonalize the individual phonon components. Using Equation 6.25 we attain the following:

$$\sum_{n=0}^{N-1} \frac{p_n^2}{2m} = \frac{1}{2mN} \sum_{k,q} p_k p_q \sum_{n=0}^{N-1} e^{i(k+q)na} = \frac{1}{2m} \sum_k p_k p_{-k} \quad (6.29)$$

Here we used the discrete nature of the lattice as given in Equation 6.26 and Equation 6.15 again. Now using Equation 6.24 we get:

$$\frac{\kappa}{2} \sum_{n=0}^{N-1} (u_n - u_{n+1})^2 = \frac{\kappa}{2N} \sum_{n=0}^{N-1} \sum_k (u_k - u_k e^{ika}) e^{ikna} \sum_q (u_q - u_q e^{iqa}) e^{iqna} \quad (6.30)$$

$$= \frac{\kappa}{2N} \sum_{k,q} (1 - e^{ika})(1 - e^{iqa}) u_k u_q \sum_{n=0}^{N-1} e^{i(k+q)na} \quad (6.31)$$

$$= 2\kappa \sum_k u_k u_{-k} \sin^2 \frac{ka}{2} \quad (6.32)$$

Here we used the cosine double-angle formula. Now we combine the two parts for the total phonon hamiltonian:

$$H_{ph} = \sum_k \left(\frac{1}{2m} p_k p_{-k} + 2\kappa \sin^2 \frac{ka}{2} u_k u_{-k} \right) \quad (6.33)$$

Define the k-dependent frequency as

$$\omega_k = \sqrt{\frac{\kappa}{m}} \sin \frac{ka}{2} \quad (6.34)$$

This gives the following simplified equation

$$H_{ph} = \frac{1}{2m} \sum_k (p_k p_{-k} + m^2 \omega_k^2 u_k u_{-k}) \quad (6.35)$$

Define the following operators

$$a_k = \frac{1}{2m\omega_k \hbar} (m\omega_k u_k + ip_k) \quad (6.36)$$

$$a_k^\dagger = \frac{1}{2m\omega_k \hbar} (m\omega_k u_{-k} - ip_{-k}) \quad (6.37)$$

The second equation is simply the Hermitian conjugate of the first. This can be seen by realizing that, because u_n and p_n are observables they must be Hermitian operators. Consider the displacement operator:

$$u_n = \sum_k u_k e^{ikx_n} = \sum_{-k} u_{-k} e^{-ikx_n} = \sum_k u_{-k} e^{-ikx_n} \quad (6.38)$$

And its Hermitian conjugate:

$$u_n^\dagger = \sum_k u_k^\dagger e^{-ikx_n} \quad (6.39)$$

Because it is Hermitian $u_n = u_n^\dagger$ which implies

$$u_k^\dagger = u_{-k} \quad (6.40)$$

A similar treatment applies to the momentum operator p_n which is also Hermitian. From this it is clear that Equations 6.36 and 6.37 are simply Hermitian conjugates of one another. As a result of these equations we come to the following:

$$u_k = \sqrt{\frac{\hbar}{2m\omega_k}} (a_k + a_{-k}^\dagger) \quad (6.41)$$

$$p_k = \frac{\sqrt{2m\omega_k \hbar}}{2i} (a_k - a_{-k}^\dagger) \quad (6.42)$$

Using these we find:

$$p_k p_{-k} = -\frac{m\omega_k \hbar}{2} (a_k a_{-k} + a_{-k}^\dagger a_k^\dagger - a_k a_k^\dagger - a_{-k}^\dagger a_{-k}) \quad (6.43)$$

$$u_k u_{-k} = \frac{m\omega_k \hbar}{2} (a_k a_{-k} + a_{-k}^\dagger a_k^\dagger + a_k a_k^\dagger + a_{-k}^\dagger a_{-k}) \quad (6.44)$$

And therefore

$$H_{ph} = \sum_k \frac{1}{2} \hbar \omega_k (a_k a_k^\dagger + a_{-k}^\dagger a_{-k}) \quad (6.45)$$

It is easy to verify that the following commutation relation is satisfied:

$$[a_k, a_k^\dagger] = 1 \quad (6.46)$$

From which it follows that

$$a_k a_k^\dagger = 1 + a_k^\dagger a_k \quad (6.47)$$

This allows us to rewrite the Hamiltonian as

$$H_{ph} = \sum_k \frac{1}{2} \hbar \omega_k (1 + a_k^\dagger a_k + a_{-k}^\dagger a_{-k}) \quad (6.48)$$

But due to the periodicity of k-space we note that

$$\sum_k (a_k a_k^\dagger + a_{-k}^\dagger a_{-k}) = 2 \sum_k a_k a_k^\dagger \quad (6.49)$$

So therefore the Hamiltonian is

$$H_{ph} = \sum_k \frac{1}{2} \hbar \omega_k (1 + 2a_k^\dagger a_k) = \sum_k \hbar \omega_k (a_k^\dagger a_k + \frac{1}{2}) \quad (6.50)$$

Electron-phonon interaction

The part of the BLF Hamiltonian which describes the electron-phonon interaction is given by:

$$H_{el-ph} = \sum_n \alpha (u_n - u_{n+1}) (c_{n+1}^\dagger c_n + c_n^\dagger c_{n+1}) \quad (6.51)$$

Using the same Fourier transformations from Equations 6.24 and 6.25 we get the following equation

$$H_{el-ph} = \frac{\alpha}{N^{\frac{3}{2}}} \sum_{n,k,q,p} u_k e^{ikna} (1 - e^{ika}) \left(c_q^\dagger e^{-iqna} e^{-iqa} c_p e^{ipna} + c_q^\dagger e^{-iqna} c_p e^{ipna} e^{ipa} \right) \quad (6.52)$$

Then by rewriting we get

$$H_{el-ph} = \frac{\alpha}{N^{\frac{3}{2}}} \sum_{k,q,p} u_k (1 - e^{ika}) \left(c_q^\dagger c_p e^{-iqa} + c_q^\dagger c_p e^{ipa} \right) \sum_n e^{i(k-q+p)na} \quad (6.53)$$

By again applying the result from Equation 6.15 we find that the last sum is equal to $N\delta_{k-q+p,0}$ which gives:

$$H_{el-ph} = \frac{\alpha}{\sqrt{N}} \sum_{q,p} u_{q-p} (1 - e^{i(q-p)a}) \left(c_q^\dagger c_p e^{-iqa} + c_q^\dagger c_p e^{ipa} \right) \quad (6.54)$$

$$= \frac{\alpha}{\sqrt{N}} \sum_{q,p} u_{q-p} c_q^\dagger c_p (1 - e^{i(q-p)a}) \left(e^{-iqa} + e^{ipa} \right) \quad (6.55)$$

$$= \frac{\alpha}{\sqrt{N}} \sum_{q,p} u_{q-p} c_q^\dagger c_p (e^{ipa} - e^{-ipa} + e^{-iqa} - e^{iqa}) \quad (6.56)$$

$$= -\frac{2i}{\sqrt{N}} \sum_{q,p} u_{q-p} c_q^\dagger c_p (\sin qa - \sin pa) \quad (6.57)$$

We now make the substitutions $p = k - \tilde{q}/2$ and $q = k + \tilde{q}/2$ which gives

$$H_{el-ph} = -\frac{2i\alpha}{\sqrt{N}} \sum_{k,\tilde{q}} u_{\tilde{q}} c_{k+\tilde{q}/2}^\dagger c_{k-\tilde{q}/2} \left(\sin((k + \tilde{q}/2)a) - \sin((k - \tilde{q}/2)a) \right) \quad (6.58)$$

$$= -\frac{4i\alpha}{\sqrt{N}} \sum_{k,\tilde{q}} \sin\left(\frac{\tilde{q}a}{2}\right) \cos(ka) u_{\tilde{q}} c_{k+\tilde{q}/2}^\dagger c_{k-\tilde{q}/2} \quad (6.59)$$

$$(6.60)$$

Where the sine addition formula was used to get to the second line. By redefining our phonon wavevector as $q = \tilde{q}$ we get the electron phonon coupling of a one-dimensional monoatomic chain to be:

$$H_{el-ph} = -\frac{4i\alpha}{\sqrt{N}} \sum_{k,q} \sin\left(\frac{qa}{2}\right) \cos(ka) u_q c_{k+q/2}^\dagger c_{k-q/2} \quad (6.61)$$

Bibliography

- [1] M. Allan, M. H. Fischer, O. Ostojic, and A. Andringa, *Creating better superconductors by periodic nanopatterning*, *SciPost Physics* **3** (2017).
- [2] J. F. Annett, *Superconductivity, Superfluids and Condensates*, Oxford University Press, New York, 1st edition, 2004.
- [3] O. Ostojic, *Metamaterial Superconductors: Proof of Principle Simulation*, Master thesis, Leiden University, 2016.
- [4] M. S. El-Bana, D. Wolverson, S. Russo, G. Balakrishnan, D. M. Paul, and S. J. Bending, *Superconductivity in two-dimensional NbSe₂ field effect transistors*, *Supercond. Sci. Technol.* **26**, 125020 (2013).
- [5] G. Ravikumar, V. C. Sahni, A. K. Grover, S. Ramakrishnan, P. L. Gammel, D. J. Bishop, E. Bucher, M. J. Higgins, and S. Bhattacharya, *Stable and metastable vortex states and the first-order transition across the peak-effect region in weakly pinned 2H-NbSe₂*, *Physical Review B* **63**, 024505 (2000).
- [6] J. Edwards and R. Frindt, *Anisotropy in the resistivity of NbSe₂*, *Journal of Physics and Chemistry of Solids* **32**, 2217 (1971).
- [7] H. Wang et al., *High-quality monolayer superconductor NbSe₂ grown by chemical vapour deposition*, *Nature Communications* **8**, 394 (2017).
- [8] J. Braspenning, *Towards Better Superconductors by Periodic Nanopatterning*, Bachelor thesis, Leiden University, 2017.
- [9] A. Andringa, *Towards Metamaterial Superconductors: A Computer Simulation*, Bachelor thesis, Leiden University, 2016.

- [10] N. W. Ashcroft and N. D. Mermin, *Solid State Physics*, Harcourt College Publishers, 1976.
- [11] H. Bruus and K. Flensberg, *Many-Body Quantum Theory in Condensed Matter Physics: An Introduction*, Oxford University Press, New York, 1st edition, 2004.

Consulted texts: [1][2][3][4][5][6][7][8][9][10][11]